FATIGUE CRACK INITIATION IN A FERRITIC-MARTENSITIC STEEL UNDER IRRADIATED AND UNIRRADIATED CONDITIONS

J. Bertsch**, A. Möslang*, H. Riesch-Oppermann*

The reduced activation steel F82H-mod of type 7-10%Cr-WVTa has been push-pull fatigue tested at 200 °C before and after homogeneous implantation of 400 appm helium to assess the lifetime of candidate fusion reactor materials. Crack initiation and propagation on carefully polished specimen surfaces were monitored by a high resolution optical microscope. Subsequent metallographic and microstructural investigations revealed crack initiation mainly along martensitic laths and transgranular crack propagation, partly affected by the orientation of martensitic bands in adjacent grains. A statistical analysis of the crack formation and propagation processes was performed. Characteristic differences between unirradiated and irradiated specimens were observed in terms of length and orientation distribution of crack segments, indicating different types of microstructural barriers for crack propagation.

INTRODUCTION

The development of structural materials with greatly reduced generation of long-lived isotopes is one of the most important challenges in fusion technology research and development. During the past years ferritic/martensitic steels of type 7-10%Cr-WVTa have been developed that satisfy not only the criteria of reduced long-term activation but show also significantly improved impact and fracture toughness properties [1,2]. The loading of structural materials in fusion reactors is, besides the plasma surface interactions, a combined effect of high heat fluxes and neutron irradiations. Next step fusion devices can be characterised by plasma burn and off-burn periods generating thermal cycling. Depending on the pulse lengths, the operating conditions, and the thermal conductivity of structural components, these oscillating temperature gradients will cause elastic and elastic-plastic cyclic deformation giving rise to (creep-)fatigue.

A specific feature of fusion neutrons is the high energy tail that leads in the next generation of fusion reactors to helium production rates of about 100 appm/y that cannot be matched adequately by conventional irradiation programs from fission reactors. Presently efforts concentrate on critical issues such as irradiation hardening at temperatures below about 300 °C and embrittlement phenomena due to helium and hydrogen. Lifetime predictions for reactor components require the generation of a suitable data base with mechanism-oriented descriptions of the fatigue damage. For these

* Forschungszentrum Karlsruhe, Institut für Materialforschung, P.O.Box 3640, D-76021 Karlsruhe, Germany
** Present affiliation: Degussa Company, Hanau, Germany

purposes, a cyclotron based irradiation programme with relevant helium accumulation was performed on suitable fatigue specimens having carefully polished surfaces. The application of a high resolution long-range optical microscope with subsequent REM and TEM analyses allows a direct correlation between crack morphology, microstructural details and fatigue data. Based on these methods, relevant results from the fracture analyses of the fatigue loaded reduced activation reference alloy F82H-mod are presented and discussed.

EXPERIMENTAL

The material used for the investigations was part of the heat F82H mod that is characterized presently within the frame of an IEA coordinated international program. The tested hollow specimens had a square cross section optimized by elastic-plastic finite element calculations, a wall thickness of 0.40 mm and a gauge length of 10 mm. The heat treatment following the fabrication consisted of 1040°C/0.5h + 750°C/1h resulting in a fully tempered martensite with carbides mainly of type $M_{23}C_6$ which lie along former austenite grain boundaries and lath boundaries. Prior to fatigue testing some of the specimens were irradiated at a blanket relevant temperature of 250 °C with a degraded 104 MeV α-particle beam to get a homogeneous concentration of 400 appm helium within the gauge volume. Continuous strain controlled cycling has been applied at 200 °C with a cycle ratio of R=-1 and a strain range between $\Delta\varepsilon_{total}$=0.4% and 0.9%.

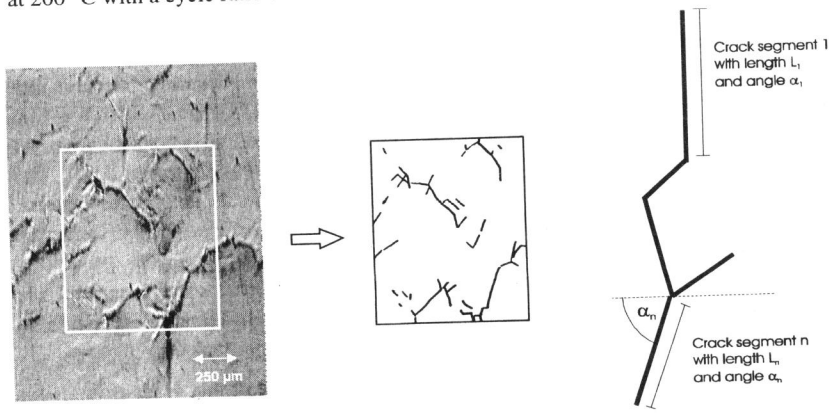

Fig. 1: Analysis and characterization of surface cracks at cycle N during strain controlled fatigue tests using a high resolution long range optical microscope.

During every fatigue test several hundred scans with a surface area of 7.0x10.0 mm^2 were recorded by triggering the camera automatically at maximum strain at a predefined cycle N. The analysis of the surface cracks was performed following the procedure of Fig. 1 by characterizing a crack or crack network as function of $N/N_{failure}$ in terms of total crack length, segment length L_n, segment density and orientation α_n with respect to the

specimen axis. To assure proper statistics, more than 20.000 crack segments have been analyzed. After fatigue testing the fatigue specimens were further investigated by metallographic methods and by scanning and transmission electron microscopy.

RESULTS AND DISCUSSION

Micro-Cracks and Structure

All specimens fatigue tested at $\Delta\varepsilon_{total}$ = 0.9% show a high density of homogeneously distributed small micro-cracks, while at smaller total strain ranges of 0.4-0.5% the density of micro-cracks is also smaller. Apart from very few exceptions micro-crack initiation and propagation is observed inside the grains, that is, the fracture behavior is completely dominated by transcrystalline cracking. Figure 2 shows clearly that the underlying microstructure has a considerable influence on the overall crack behavior. Practically all micro-cracks are oriented along Cr-rich precipitates mainly of type $M_{23}C_6$. These very fine secondary precipitates were formed at inner surfaces during the final heat treatment, that is, at grain and in the vast majority at lath boundaries. Microstructural barriers and the orientation of the martensite lath packages play an important role for the crack growth behavior. Often micro-cracks stop e.g at a grain boundary as figure 2 (left side) shows. The propagation of a micro-crack into an adjacent grain or lath package is usually accompanied by a change of the crack orientation. A typical example for such a behavior is illustrated in fig. 2 (right side).

Orientation Distribution of Crack Segments

It became obvious during the crack pattern analyses that the orientation of the cracks is not uniformly distributed although the orientations of the martensite laths and consequently the rows of the segregated $M_{23}C_6$ precipitates are completely isotropic as careful statistical investigations have shown. With respect to the orientation distribution, the micro-cracks of both, irradiated and unirradiated specimens, can be classified into two categories (i) low $\Delta\varepsilon_t$ and (ii) high $\Delta\varepsilon_t$. This classification is based on a determination

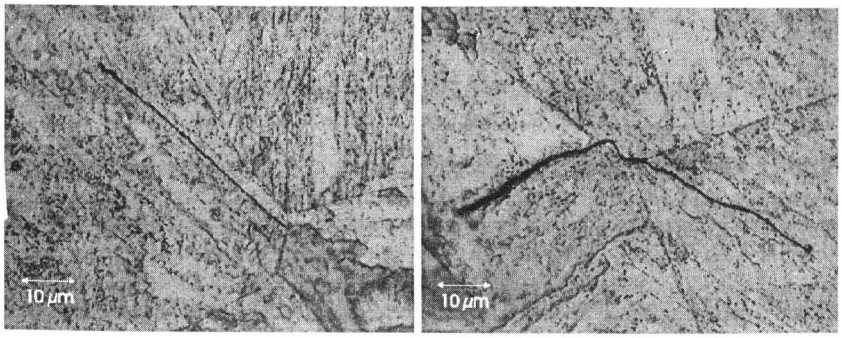

Fig. 2: Micrographs showing micro-cracks oriented along rows of $M_{23}C_6$ precipitates. Crack arrest (left side) and change of direction (right side) at a boundary.

of the angle α_n between crack segment and load axis in steps of 10 degrees and is weighted according to the related accumulated segment length.

(i) Low total strain ranges (0.4-0.5%): After intrusions and extrusions have been developed, crack initiation starts slowly between N/N_f = 0.1and 0.2 with a pronounced maximum between 40 and 50 degree (fig. 3). Obviously an angle consistent with 45° which describes the orientation of maximum shear stress in the continuum is clearly preferred in this case. A specific feature in fig. 3 is the network formation of cracks beyond about 30000 cycles which results in a relative high population of small angles due to vertical coupling of adjacent cracks. It is important to note, that at low strain ranges and perfectly polished specimen surfaces, micro-crack initiation starts practically without exception on intrusions and extrusions that develop in a first step in the direction of maximum shear stress along suitably oriented lath boundaries.

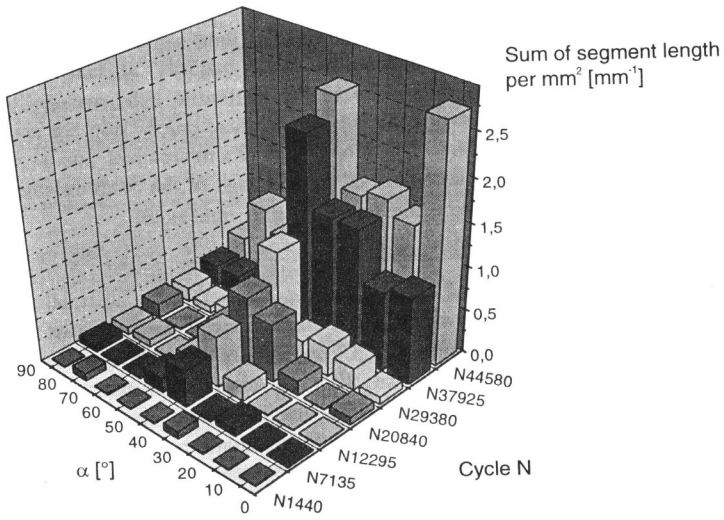

Fig. 3: Distribution of segments as function of cycle number and angle to load axis for an unirradiated specimens tested at $\Delta\varepsilon_t$ = 0.44%.

(ii) High total strain ranges (0.8-0.9%): After a few cycles micro-crack initiation and propagation start with an orientation maximum of crack segments between 50 and 60 degree. This maximum can be interpreted in a natural way by a superposition of two different crack initiation processes. The first one is the already mentioned shear stress driven plastic deformation along lath boundaries oriented close to 45 degree, while the second component can be attributed to interface separation induced by normal stress that has its maximum at 90 degree. At higher strain ranges the local stress and the related plastic deformation are obviously sufficient for interface separation e.g. between primary precipitates and the matrix.

Growth of Micro-Cracks

The formation of branched cracks starts always with the development of individual cracks, that is, at the beginning of fatigue testing one crack corresponds to a single segment. In a second step either crack initiation increases the number of single cracks or the cracks propagate by keeping a low segment production rate. Depending on the total stain range and microstructural modifications prior to fatigue testing e.g. by irradiation, either mechanism can dominate. If single cracks start to coalesce or if the segment density is very high, crack interaction can no longer be neglected. This is why in this study the analysis is concentrated on crack segments and individual cracks rather than on the investigation of crack networks. Figure 4 shows the spatial density of crack segments as function of the normalized fatigue life for both low and high total strain amplitudes. Obviously at high strain ranges already in the early stage of fatigue testing a high density of cracks segments is formed followed by network formation, while at low strain amplitudes a low segment density is kept over more than 70% of the fatigue life.

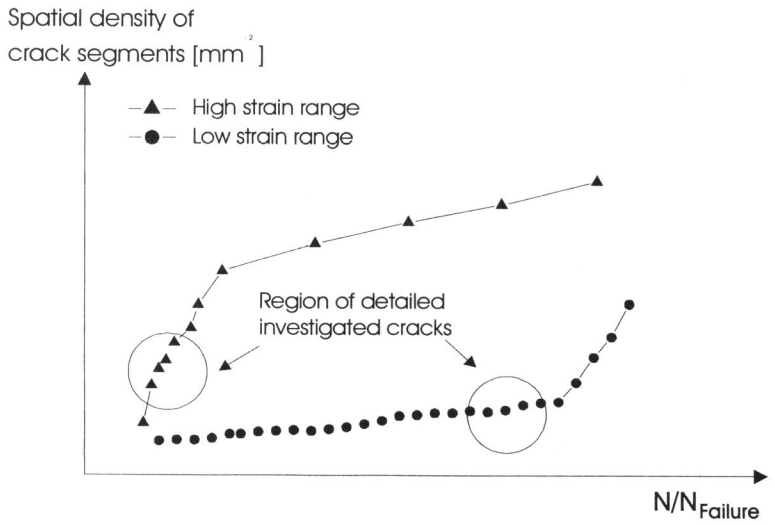

Fig. 4: Regions of well developed individual cracks before network formation starts.

The present investigations of the ferritic/martensitic steel F82H-mod confirm the general consensus of data published on many other materials [3], that during the initial phase of fatigue testing small micro-cracks are formed with high crack growth rates in unirradiated specimens independent of the strain range as shown in fig. 5. Once the segment length has reached 75(±10) μm, which corresponds closely to the mean grain diameter of this material, the crack stops or changes the direction. That is, within the whole strain range the micro-crack morphology in the unirradiated condition is largely controlled by microstructural barriers.

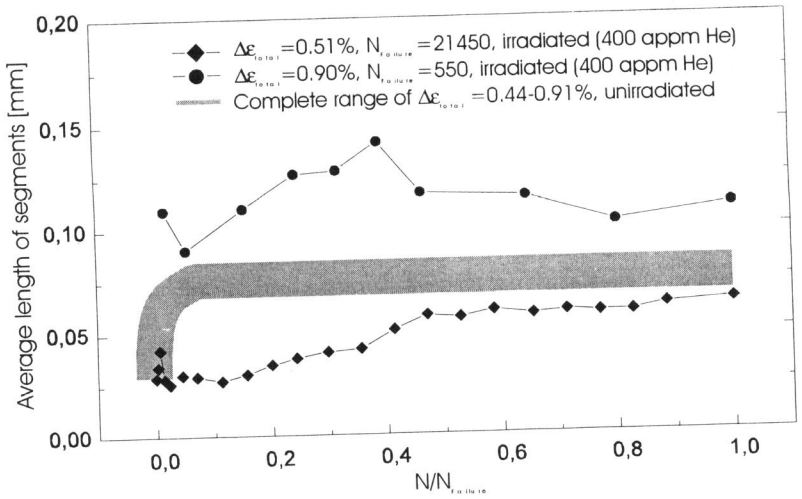

Fig. 5: Effect of strain range and pre-implantation of 400 appm helium at 250 °C on the fatigue crack growth behavior of the ferritic/martensitic steel F82H-mod.

The behavior of irradiated specimens, is quite different as fig. 5 shows. At high strain ranges microstructural barriers are surmounted already during the first few cycles and early network formation of cracks follows resulting in fatigue life reduction by a factor 5-7. In this case the early formation of cracks can be attributed to an increase of the total stress amplitude of almost 200 MPa [4,5] due to irradiation hardening. However, at small $\Delta\varepsilon_{total}$ the total stress amplitude of irradiated and unirradiated specimens is not very different. In this case, the growth of micro-cracks is impeded by very small irradiation induced defects (e.g. dislocation loops, helium bubbles, defect clusters) before they are able to reach barriers like grain and lath boundaries. A more detailed correlation between crack morphology, microstructural features and fatigue properties will be presented in a forthcoming publication.

REFERENCES

[1] A. Koyama, A. Hishinuma, D.S. Gelles, R.L. Klueh, W. Dietz, K. Ehrlich, J. Nucl. Mater. 233-237 (1996) 138-147.

[2] K. Ehrlich, D.R. Harries, A. Möslang, „Characterization and Assessment of Ferritic/Martensitic Steels", Report FZKA 5626 (Febr. 1997).

[3] L.A. James: Fatigue crack propagation in austenitic steels, Atomic Energy Review 14 (1976) 37-85.

[4] R. Lindau, A. Möslang, J. Nucl. Mater. 212-215 (1994) 599.

[5] J. Bertsch, R. Lindau and A. Möslang J. Nucl. Mater. 233-237 (1996) 276.